Stochastic Resonance to Control Diffusive Motion in Chemistry

Damien Alcor,[†] Jean-François Allemand,[†,‡] Emmanuelle Cogné-Laage,[†] Vincent Croquette,*[,‡] Fabien Ferrage,[§] Ludovic Jullien,*[,†] Alexeï Kononov,[†] and Annie Lemarchand*[,||]

École Normale Supérieure, Département de Chimie, C.N.R.S. U.M.R. 8640, 24, rue Lhomond, 75231 Paris Cedex 05, France, École Normale Supérieure, Département de Physique, C.N.R.S. U.M.R. 8550, 24, rue Lhomond, 75231 Paris Cedex 05, France, École Normale Supérieure, Département de Chimie, C.N.R.S. U.M.R. 8642, 24, rue Lhomond, 75231 Paris Cedex 05, France, and Université Pierre et Marie Curie, Laboratoire de Physique Théorique des Liquides, C.N.R.S. U.M.R. 7600, 4, place Jussieu, 75252 Paris Cedex 05, France

Received: July 16, 2004; In Final Form: October 28, 2004

This paper reports on a novel procedure to tune the effective diffusion coefficient of a field-sensitive reactant in the presence of a periodic external field. We investigate the motion of two negatively charged azo dyes interacting with α-cyclodextrin (α-CD) upon action of a periodic square wave electrical field. We show that the dyes exhibit an effective diffusion coefficient D_{eff} that depends on the rate constants for dye complexation within α-CD, the period and the amplitude of the field. UV−vis absorption, gradient field ^{1}H NMR, and fluorescence correlation spectroscopy (FCS) after two photon excitation are used to evidence that D_{eff} may be increased far beyond its intrinsic value when specific relations interpreted as a stochastic resonance are fulfilled. The present results may find useful applications in chemical kinetics as well as for molecular sorting.

1. Introduction

External fields may alter the energetic features of reactants: Modifications of chemical compositions or molecular motions can be obtained.[1] For instance, electrolysis and electrophoresis are familiar phenomena originating from the change of the chemical potential of an ion upon the application of an electric field.[2,3] Pulse or periodic field modulation can give access to kinetic information.[4,5] In the present paper, we explore a novel phenomenon originating from coupling a chemical reaction with a periodic external field: the effective diffusion coefficient of a field-sensitive reactant can be selectively enhanced when its average lifetime and the period of the alternating field are matched.

In the following, we consider a system under the chemical reaction 1

$$P + C \underset{k_2}{\overset{k_1}{\rightleftharpoons}} Q \qquad (1)$$

in the presence of a periodic field $\vec{E}$ with null average value like $E = a \sin(2\pi t/T)$ where T is the field period. Such associative processes are common in Chemistry and Biology (formation of host−guest or ligand receptor complexes, pairing between single stranded-DNA, ...). C and/or Q are supposed to be field-sensitive and P is a third reactant. Introducing the extent of reaction 1, $\xi(t)$, the field oscillation induces a modulation of the chemical composition around its equilibrium value $\xi_\infty(a = 0)$ in the absence of field: $\xi(t) = \xi_\infty(a = 0) + \bar{\xi} \sin(2\pi t/T - \phi)$ where ϕ is a phase lag. This oscillation also forces a periodic motion of the molecules C and Q. At low enough field frequency, many exchanges between the reactants and the products take place in average before any significant change of the chemical potentials occurs: $\xi(t)$ has enough time to relax to its instantaneous equilibrium value and $\phi \simeq 0$. In relation to molecular motion, fast exchange between C and Q allows us to consider that the system contains a virtual (C, Q) component[5] whose field-sensitivity is determined from appropriately averaging the field-sensitivity of C and Q. In contrast, no chemical exchange takes place in average at high enough field frequency. Under such conditions, the composition of the system remains identical to that in the absence of the field-induced perturbation: $\bar{\xi} = 0$. The positions of C and Q now evolve independently, in relation with their own field-sensitivity. The field frequency marking the transition between the two preceding regimes manifests itself as a threshold in the $\bar{\xi}(T)$ curve.[4,5] This characteristic frequency leads to the relaxation time toward equilibrium via reaction 1 that can be subsequently used to extract rate constants.[4] As soon as the beginning of the 19th Century, Debye analyzed the reorientation of dipolar molecules using an alternating electric field.[6,7] Then Wien, Onsager, and Eigen relied on a similar approach to investigate the kinetics of reactions involving ions.[4,8−10]

The preceding frame found a renewed interest in the context of stochastic resonance.[11,12] In relation with applying a periodic field on a reactive system submitted to a chemical reaction such as 1, initial claims for stochastic resonance mainly emphasized on the dependence of the amplitude of the extent $\bar{\xi}(T)$ on the noise level.[12] First evidences for stochastic resonance in chemistry were observed along this line in continuously stirred tank reactors submitted to reactions known to exhibit complex

* To whom correspondence should be addressed. (L.J.) Fax: (+33) 1 44 32 33 25. E-mail: Ludovic.Jullien@ens.fr. (V.C.) Fax: (+33) 1 44 32 34 92. E-mail: Vincent.Croquette@ens.fr. (A.L.) E-mail: anle@lptl.jussieu.fr.

† C.N.R.S. U.M.R. 8640.

‡ C.N.R.S. U.M.R. 8550.

§ C.N.R.S. U.M.R. 8642.

|| C.N.R.S. U.M.R. 7600.

10.1021/jp0468307 CCC: $30.25
Published on Web 12/31/2004

mechanisms.[13−18] The notion of stochastic resonance has been subsequently extended to other situations.[19,20] In relation to chemistry, stochastic resonance has been thus considered for separation applications.[21,22] Attention is now paid on the motion of reactants determined by a periodic field. In classical chromatography, a constant field induces the motion of mixture components that are separated according to their affinity for the chromatography medium. During the separation, all of the molecules of a given component do not experience identical individual trajectories and they are dispersed in the course of time around an average position: peaks are broadened. The corresponding phenomenon has been extensively covered both theoretically[23−39] and experimentally.[40−42] In contrast, the dispersion of reactive particles suspended in time-periodic flows was only theoretically investigated.[19−21,43,44] In particular, it was predicted that dispersion is maximal if the time scales associated with the stochastic process, here the chemical reaction, are close to the half-period of the electric field. This paper reports on the first experimental observation of a stochastic resonance in a chemical system involving a "simple" reaction. Such a result is especially significant to devise a novel chromatography procedure adapted to the selective extraction of a given reactant from a mixture.[45]

The present paper is organized as follows. In section 2, we sum up the relevant theoretical results dealing with dispersion of a reactant in a periodic field. A more general development than in ref 21 is given in the Supporting Information. To check the theoretical prediction for the effective dispersion coefficient, the different parameters characterizing the model system are determined in section 3. We then report on the dispersion observed in a tailored stochastic resonance regime. Section 4 is devoted to conclusions.

2. Theoretical Results

We consider a one-dimensional (1D) reaction−diffusion system submitted to a uniform, time-periodic (pulsation ω, period T), field (electric in the following). C is supposed to react with a target P, producing Q, according to reaction 1 where the rate constants k_1 and k_2 are respectively associated with the forward and backward reaction. $K = k_1/k_2$ designates the association constant. The concentration of species P is assumed to be uniform and in excess.

One assumes that C is initially introduced at a given point of the medium chosen as the origin. The motion of C and Q becomes diffusive after a short transient regime (see the Supporting Information). More precisely, beyond the relaxation time of the chemical reaction 1 $\tau_\chi = 1/(\kappa_1 + k_2)$ ($\kappa_1 = k_1P$), C and Q entered in a regime of fast exchange making relevant the notion of virtual[5] species (C, Q). Under these conditions, the variance of the concentration profile $C(x, t) + Q(x, t)$ reduces to $\sigma_{(C,Q)}^2(t) = 2D_{\text{eff}}t$ with

$$D_{\text{eff}} = D_{\text{diff}} + D_{\text{disp}} \tag{2}$$

where

$$D_{\text{diff}} = \frac{1}{(1+KP)}D_C + \frac{KP}{(1+KP)}D_Q \tag{3}$$

and

$$D_{\text{disp}} = [a(\mu_C - \mu_Q)]^2 \frac{\kappa_1 k_2}{(\kappa_1 + k_2)^3}\left[\frac{1}{2\left(1+\left(\frac{\omega}{\kappa_1+k_2}\right)^2\right)}\right] \tag{4}$$

for a sinusoidal electric field of the form $E(t) = a\sin(\omega t)$ whereas

$$D_{\text{disp}} = [a(\mu_C - \mu_Q)]^2 \frac{\kappa_1 k_2}{(\kappa_1 + k_2)^3}\left[1 - \frac{4}{(\kappa_1+k_2)T}\frac{1-\exp(-(\kappa_1+k_2)T/2)}{1+\exp(-(\kappa_1+k_2)T/2)}\right] \tag{5}$$

for a square-wave electric field of period T obeying, for n integer[46]

$$E(t) = a,\ nT \le t < (n+1/2)T$$
$$E(t) = -a,\ (n+1/2)T \le t < (n+1)T \tag{6}$$

D_C and D_Q and μ_C and μ_Q designate the diffusion coefficients and the electrophoretic mobilities of C and Q respectively.

The effective diffusion coefficient D_{eff} contains two terms. The diffusive term D_{diff} originates from coupling between the chemical reaction 1 and the Brownian diffusion. The dispersive term D_{disp} comes from the dispersion of the profile of the (C, Q) concentration induced by coupling between the chemical reaction 1 and the field.

The expressions of D_{disp} given in (4) and in (5) are symmetric functions of κ_1 and k_2. Provided that species C and Q have different electrophoretic mobilities μ_C and μ_Q, D_{disp} can reach any arbitrarily large value by adjusting the amplitude a of the electric field. At fixed P and T, D_{disp} considered as a function of κ_1 and k_2 exhibits a single maximum. For a sinusoidal field, this maximum is given by

$$\kappa_1^R = k_1^R P = k_2^R = \omega/2 = \pi/T \tag{7}$$

whereas it obeys

$$\kappa_1^R = k_1^R P = k_2^R \simeq 3.212/T \tag{8}$$

in the case of a square-wave field. As displayed in Figure 1a, modifying the rate constants by only 1 order of magnitude is sufficient to induce a considerable drop of D_{disp}. For a given set of rate constants $\{k_1, k_2\}$, there is an upper limit for the field pulsation to couple chemistry and the field; D_{disp} essentially differs from zero when $\omega \le \kappa_1 + k_2$ for an appropriate range of the P concentration (Figure 1b).

The maxima given by the relations 7 and 8 are interpreted as stochastic resonances (as indicated by the exponent R). Stochastic resonance was first experimentally evidenced as well as theoretically understood in the context of bistable systems exhibiting a stochastic hopping process when they are submitted to an appropriate periodic forcing.[12] Then the concept of stochastic resonance was extended to different physical situations to account for the observation of nonmonotonic behaviors when the time scales associated to a stochastic process and to an external forcing are matched.[20] Here, such a singular behavior (maximum of D_{eff}) precisely results from the optimization of the stochastic exchange process between C and Q, and the periodic field. In principle, the present system involves three phenomena: (i) the intrinsic diffusion; (ii) the forward and backward reactions 1, characterized by the two average lifetimes of the free and bound states: $\overline{\tau_C} = 1/\kappa_1$ and $\overline{\tau_Q} = 1/k_2$; (iii) the periodic electric field of period T. The intrinsic diffusion is negligible at large field amplitude. Stochastic resonance can be here observed even in the absence of external noise. In fact, chemical reactions are intrinsically random processes the underlying stochastic nature of which is here revealed at the

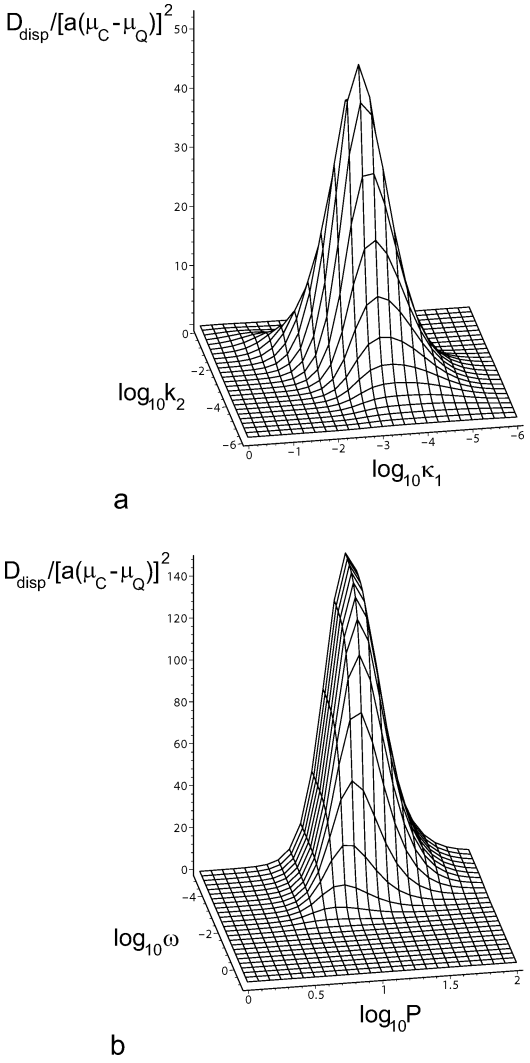

Figure 1. Theoretical variation in the normalized dispersive coefficient $D_{disp}/[a(\mu_C - \mu_Q)]^2$ of species (C, Q) submitted to a sinusoidal periodic field ($E(t) = a \sin(\omega t)$) in logarithmic units with (a) $\kappa_1 = k_1 P$ and k_2 ($\omega = 0.002$) and (b) ω and P ($k_1 = 0.0001$ and $k_2 = 0.001$).

macroscopic level by the dispersion phenomenon. The dispersion coefficient D_{disp}, considered as a function of the rate constants κ_1 and k_2, is maximum when the two time scales associated with the random processes are close to the half-period of the field, as expressed by relations 7 and 8.

Qualitatively, this stochastic resonance is understood as follows.[20,21] As in the standard system where stochastic resonance has been first investigated, the system contains two states: C and Q that exhibit a different sensitivity to the field. Thanks to reaction 1, the molecules undergo random jumps between the state C and the state Q. We first assume that the lifetimes of all of the molecules of a given type are equal to their average lifetime. We consider a molecule that is initially in the state C. During the first half period $T/2$ of the field, the molecule moves at a velocity $a\mu_C$. If $T/2 \approx \overline{\tau_C} = 1/\kappa_1$ (condition 1), then the molecule converts into the state Q moving at the velocity $a\mu_Q$ due to reaction 1 when the field changes of sign. If $T/2 \approx \overline{\tau_Q} = 1/k_2$ (condition 2), the molecule comes back again in state C when the field adopts its initial orientation at the end of the second half period. Hence, the distance travelled during the first half period by the molecule in state C is not retraced back by the molecule in the state Q during the second half period: the molecule moved by $\Delta x = a(\mu_C - \mu_Q)T$ during one period T. Due to the absence of synchronization of the

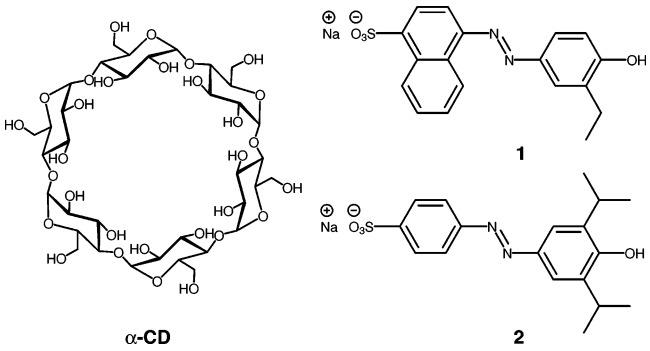

Figure 2. Molecular formulas of the chemical species investigated.

molecules within the ensemble as well as the Poisson distribution of the molecular lifetimes, an isotropic dispersion is observed instead of an oriented motion: At the single molecule level, a molecule exchanging between the states C and Q whose rate constants obey relations 7 and 8 only keeps the same direction of motion for a longer time than another that is not resonant. Then the dispersive contribution to the effective diffusion coefficient is associated to a dispersion coefficient $(\Delta x)^2/T \approx [a(\mu_C - \mu_Q)]^2/k_2^R$ the scaling of which is in fair agreement with the derivation obtained by taking into account the eqs 4−8.

3. Experimental Results and Discussion

Presentation of the System. An electric field was used in the present study. Consequently, we look for a process obeying eq 1 that involves charged species exhibiting different electrophoretic mobilities. Complexation of a negatively charged azo dye denoted **i** (**i** = **1** for 3′-ethyl-4′-hydroxyphenylazo-1-naphthalene-4-sulfonate and **i** = **2** for 3′,5′-diisopropyl-4′-hydroxyphenylazo-1-benzene-4-sulfonate) by α-cyclodextrin (α-CD) was chosen (Figure 2 and eq 9)[47−50]

$$\alpha\text{-CD} + \mathbf{i} \underset{k_{i,2}}{\overset{k_{i,1}}{\rightleftharpoons}} i\subset \alpha\text{-CD} \qquad (9)$$

In relation with the model exposed above, the dye **i** and the complex $i \subset$ α-CD play the respective roles of C and Q whereas α-CD acts as P.

A first series of experiments was directed to determine the charges of the dyes **i** and the complexes $i \subset$ α-CD under basic conditions (pH = 11−12) where both thermodynamic and kinetic information was available.[47,48] Both azo dyes **1** and **2** contain two ionizable acidic groups. The second protonation constants $pK_{a,2}$(i) originating from the phenol group were determined for 1 and 2 by titration followed by UV−vis absorption (Figures 1S and 2S). The observed values, 8.3 ± 0.2 for **1**, and 8.2 ± 0.2 for **2**, agree well with the dye structures.[51] Question arose whether the second protonation constants of the encased dyes $pK_{a,2}(i \subset$ α-CD) considerably differ from the corresponding values for **i**. Indeed, the low dielectric constant within the α-CD cavity could induce some increase with regards to the corresponding $pK_{a,2}$ in water.[52,53] Although no direct determinations of $pK_{a,\,2}(i \subset$ α-CD) were undertaken, the charges of the $i \subset$ α-CD complexes at pH = 11−12 were deduced from consideration of their UV−vis absorption spectrum. A large blue shift (≈100*nm*) of the absorption band of the dyes accompanies the neutralization of the phenate group (see Figures 1S and 2S). No such shift was observed in the UV−vis absorption spectrum of the azo dyes upon complexation within the α-CD cavity under the reported basic conditions.[47,48] In fact, complexation determines a slight red shift that could not be explained by any solvatochromic

TABLE 1: Thermodynamic and Kinetic Information Related to Complexation of the Azo Dyes 1 and 2 by α-CD at 298 and at 283 K as Extracted from the Literature

i	$k_{i,1}(298)$ ($M^{-1}s^{-1}$)	$k_{i,2}(298)$ (s^{-1})	$K_i(298)$	$k_{i,1}(283)$ ($M^{-1}s^{-1}$)	$k_{i,2}(283)$ (s^{-1})	$K_i(283)$
1[a]	6.0	3.5×10^{-2}	171	2.1	6.3×10^{-3}	340
2[b]	3.5 10^2	0.5	700	1.0×10^2	0.1	1000

[a] These values have been derived from the data given in reference 47. The original values were measured in a phosphate buffer at pH = 11.5 (ionic strength: 0.1 M) at 287 ± 1 K: $k_1(287\ K) = 2.8\ M^{-1}\ s^{-1}$, $k_2(287\ K) = 1.010^{-2}\ s^{-1}$ and $K(287\ K) = 280$. We used the reported values of the enthalpy ($\Delta_r H^\circ = -32.2\ kJ\ mol^{-1}$) and of the activation energy ($E_a = 49.0\ kJ\ mol^{-1}$) for complex formation to extrapolate the corresponding values at 298 K from the Arrhenius equation. [b] These values are given in reference 48. They were measured at pH = 11.8−12 (NaOH; ionic strength fixed by NaCl addition: 0.1 M) at 298 ± 1 K. We used the reported values of the enthalpy ($\Delta_r H^\circ = -21.9\ kJ\ mol^{-1}$) and of the activation Gibbs free energy ($\Delta_r G^{0\neq} = 58.5\ kJ\ mol^{-1}$) for complex formation to extrapolate the corresponding values at 283*K*.

TABLE 2: Thermodynamic and Kinetic Information Related to Complexation of the Azo Dyes 1 (at 298 K) and 2 (at 283 K) by α-CD as Evaluated in the Present Study at 0.15 M Ionic Strength (See Text and Experimental Section)

i	K_i	$k_{i,1}$ ($M^{-1}s^{-1}$)	$10^2 k_{i,2}$ (s^{-1})	$k_{i,1}/k_{i,2}$ (M^{-1})
1	100,[a] (50, 90),[b] 170[c]	6.1,[d] 7.0,[e] 5.1[f]	3.5,[d] 3.1,[e] 4.0[f]	175,[d] 225,[e] 127[f]
2	1200,[a] 1600[c]	125[f]	18[f]	700[f]

[a] Measured in solution during titrations followed by UV−vis absorption. Values are given ±30 for **1** and ±700 for **2**. [b] Determined from averaging the suitable integrals during ^{1}H NMR experiments respectively in the absence or in the presence of 1% agarose. [c] Extracted from fitting the velocities of the front migrations of the dyes **i**. [d] Extracted from fitting the effective diffusion coefficient of the dye **1** as a function of the field amplitude. [e] Extracted from fitting the effective diffusion coefficient of the dye **1** as a function of the field period. [f] Extracted from fitting the effective diffusion coefficient of the dyes **i** as a function of concentration in α-CD.

effect exerted by the α-CD cavity on the protonated dyes (see Figures 3S and 4S). Eventually, one anticipates the absence of α-CD ionization below pH = 12.3 which is reported as the first pK_a of α-CD.[54] Thus **1**, **2**, *1* ⊂ α-CD and *2* ⊂ α-CD were all doubly negatively charged at pH = 11. This pH value was chosen for the subsequent experiments. Consequently, the difference between the mobilities of C and Q does not result here from the charge but from the size.

To validate our theoretical model, the relevant kinetic and thermodynamic information related to reaction 9 were needed. We used reported data to derive the corresponding constants under different experimental conditions.[47,48] Results are given in Table 1. The following experiments relying on direct observation of migration/diffusion of the dyes in glass capillaries were performed in 1% agarose gels to avoid electrosmosis that could overcome the specific effects expected. In principle, no major change of the preceding kinetic and thermodynamic features were anticipated at such a low concentration in agarose. Indeed, typical pore size should be about 400 nm that is much larger than the molecular size of the chemical species involved in reaction 9.[55] Nevertheless, we compared the thermodynamic constants K_i associated to reaction 9 either in solution (titration followed by UV−vis absorption and evaluation from ^{1}H NMR) or in the gel (evaluated from ^{1}H NMR) to examine the possible influence of the gel (Figures 3S and 4S). Results are given in Table 2. The K_i values determined in solution satisfactorily compare with the derivations made above from the literature (see Table 1). In addition, the values measured in solution and in the gel do not significantly differ. In fact, the observed changes remain much lower than one order of magnitude which offers good conditions for the evaluation of the theoretical predictions (vide supra).

Preliminary Experiments. Experiments were first directed to determine the relevant parameters for analyzing the effective diffusion coefficients obeying eq 2. Once the rate and thermodynamic constants associated with reaction 9 are known (vide supra), one has to measure (i) the intrinsic diffusion coefficients, D_i and $D_{i\subset\alpha-CD}$, and electrophoretic mobilities, μ_i and $\mu_{i\subset\alpha-CD}$, of the different species involved; (ii) the amplitude a of the electric field. One also has to be concerned with the dependence of the medium viscosity on the concentration in α-CD, i.e., the dependence of the diffusion coefficients and the electrophoretic mobilities on the concentration in α-CD.

Dependence of Solution Viscosity upon α-CD *Concentration.* The relative dependence of medium viscosity as a function of α-CD concentration, $\eta([\alpha\text{-CD}])$, was approached by two different methods. The first one was based on investigating the dependence of the current intensity $I([\alpha\text{-CD}])$ in the electrophoretic cell on α-CD concentration. In fact, I is inversely proportional to the medium viscosity (see the Experimental Section). In addition, we investigated the dependence of the diffusion coefficient $D^*([\alpha\text{-CD}])$ of a suitable fluorescent label as a function of α-CD concentration. Indeed, diffusion coefficients are inversely proportional to medium viscosity (see the Experimental Section). Fluorescein was chosen in relation with its structural similarity with the investigated azo dyes. In principle, one thus anticipates eq 10

$$\frac{\eta([\alpha\text{-CD}])}{\eta([\alpha\text{-CD}]=0)} = \frac{I([\alpha\text{-CD}]=0)}{I([\alpha\text{-CD}])} = \frac{D^*([\alpha\text{-CD}]=0)}{D^*([\alpha\text{-CD}])} \quad (10)$$

The results are displayed in Supporting Information (Figure 5S). The data directly obtained by gradient field ^{1}H NMR on the dyes were also added in Figure 5S. All of the data are in satisfactory agreement. The relative viscosity increases as a function of α-CD concentration. In the investigated range $0-5.8 \times 10^{-2}$ M, it obeys the empirical function given in eq 11

$$\frac{\eta([\alpha\text{-CD}])}{\eta([\alpha\text{-CD}]=0)} = 1.00 + 8.0[\alpha\text{-CD}] - 68[\alpha\text{-CD}]^2 \quad (11)$$

At 6×10^{-2} M, medium viscosity is increased by 20%.

Determination of the Diffusion Coefficients of the Dyes i. The diffusion coefficients were measured by direct observation of the relaxations of step profiles of concentration in a transparent electrophoretic cell with a camera (Figure 3, parts a and b). Details about recording and analyzing the signals are described in the Experimental Section and in Figure 6S. The experiments were respectively performed at 298 K for **i** = **1**, and at 283 K for **i** = **2** (vide infra). The intrinsic diffusion coefficients D_i of the dyes **i** were evaluated in the absence of electric field. D_1 was also measured in the presence of a strong square wave periodic field, far from the resonance conditions obeying eq 8 (U_{app} = 100 V, [α-CD] = 0 M, T = 90 *s*). Results are given in Table 3. Comparative measurements were also performed by pulse field gradients (PFG) ^{1}H NMR, in solution and in the agarose gel. The results are also given in Table 3 and complementary data are available as Supporting Information (Table 1S).

Comparison between the data acquired in solution and in the gel by PFG ^{1}H NMR underlines that the agarose gel does not induce any large alteration of the diffusion coefficients of the

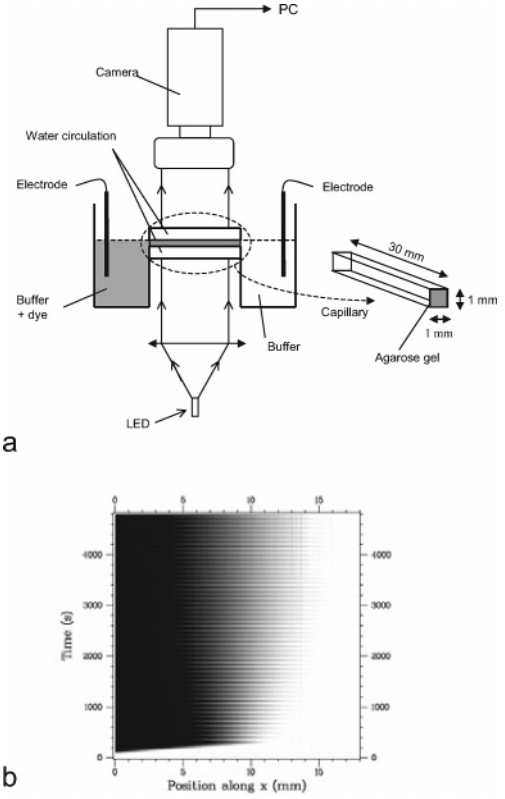

Figure 3. (a) Instrumental setup used for determining the electrophoretic mobilities and the diffusion coefficients of the azo dyes; b: Typical record of a diffusive profile as a function of time. We record the transmitted image from a thin channel parallel to the capillary containing the dye (*x* axis) as a function of time (*y* axis). The dye absorbs the light emitted by the LED; it is thus located in the dark region of the recorded image. The dye is introduced at the left of the picture. A constant electric field is first applied to locate the front of the concentration profile of the dye close to the center of the image. The electric field is then switched to become periodic. One notices both a ratchet motion of the front and a diffusion of the profile.

TABLE 3: Diffusion Coefficients of the Azo Dyes i and of Their Complexes with α-CD in 1% Agarose Gel at 298 K for 1 and 283 K for 2 as Measured by Direct Observation and Gradient Field H^1 NMR (See Text and Experimental Section)

i	D_i (10^{-10} m^2 s^{-1})	$D_{i\subset\alpha-CD}$ (10^{-10} m^2 s^{-1})
1	3.9,[a] 4.1,[b] 3.8,[c] 4.1,[d] (4.9)[e]	2.0,[c] 2.6,[d] (3.0)[e]
2	2.5,[a] −, 2.5,[c] 2.2,[d] (2.3)[e]	0.9,[c] 1.4,[d] (1.6)[e]

[a] Derived from observing the relaxation of a concentration step in the absence of electric field. [**i**] = 0.3 mM. Precision: $\pm 10^{-10}$ m^2 s^{-1}. [b] Derived from observing the relaxation of a concentration step in the presence of a strong periodic square wave field far from the resonance conditions obeying eq 8. [**1**] = 0.3 mM, U_{app} = 100 V, [α-CD] = 0 M, T = 90 s. Precision: $\pm 10^{-10}$ m^2 s^{-1}. [c] Derived from observing the relaxation of a concentration step in the absence of electric field. [**i**] = 0.3 mM; [α-CD] = 5.8 mM for **1**, and [α-CD] = 1.0 mM for **2**. Precision: $\pm 10^{-10}$ m^2 s^{-1}. [d] Derived from PFG H^1 NMR. [**1**] = 5 mM, [**2**] = 5 mM; pH = 12, 0.15 M ionic strength. In the presence of α-CD, [α-CD] = 8.3 mM for the experiment performed with **1**, and [α-CD] = 1.0 mM for the experiment performed with **2**. Precision: $\pm 0.110^{-10}$ m^2 s^{-1}. [e] Derived from PFG H^1 NMR in the absence of agarose gel. [**1**] = 5 mM, [**2**] = 5 mM; pH = 12, 0.15 M ionic strength. In the presence of α-CD, [α-CD] = 8.3 mM for the experiment performed with **1**, and [α-CD] = 1.0 mM for the experiment performed with **2**. Precision: $\pm 0.110^{-10}$ m^2 s^{-1}.

dyes; whatever the molecular probe used, the gel-induced increase of viscosity is limited to the range 10% to 20% (See Tables 3 and 1S. See also Figure 5S in the Supporting Information). These observations are in line with the evaluations of the association constants suggesting that the agarose gel does not lead to major alterations of the behavior observed in solution (vide supra). The results obtained by PFG ^{1}H NMR compare well with the values measured by observing the relaxation of step profiles of dye concentration; the corresponding agreement can be considered to validate both our setup and the data treatment to extract the diffusion coefficients. As anticipated from eq 2, the diffusion coefficients measured either in the absence of electric field or in the presence of a strong alternating field far from the resonance conditions do not differ. In addition, the corresponding comparison suggests that the interaction of the substrates with the agarose matrix does not promote any significant dispersion.

In view of the low concentration of dyes during these series of experiments, the latter values of the diffusion coefficients can be considered as directly relevant for evaluation of the theoretical model developed above. We retained $D_1^0(298\ \mathrm{K}) = 4.0 \pm 1 \times 10^{-10}$ m^2 s^{-1} and $D_2^0(283\ \mathrm{K}) = 2.4 \pm 1 \times 10^{-10}$ m^2 s^{-1}. In the following, the zero in exponent refers either to the absence or to the extrapolation to null concentration of α-CD.

Determination of the Diffusion Coefficients of i ⊂ α-CD. The extrapolated values of the diffusion coefficients $D^0_{i\subset\alpha-CD}$ of the $i \subset$α-CD complexes at null concentration of α-CD were independently evaluated from two series of experiments. The diffusion of the dyes **i** in media containing α-CD at a concentration equal to $1/K_i$ was first investigated by the observation of the relaxation of a step profile of concentration in i. Under such conditions, one measures $D_{diff} = (D_i^{[\alpha-CD]=1/K_i} + D_{i\subset\alpha-CD}^{[\alpha-CD]=1/K_i})/2$ (see eq 3). $D_i^{[\alpha-CD]=1/K_i}$ can be evaluated by correcting the D_i^0 value determined above from the viscosity dependence on [α-CD] given in eq 11. Then $D_{i\subset\alpha-CD}^{[\alpha-CD]=1/K_i}$ can be extracted. The results are displayed in Table 3. Measurements were also performed by PFG ^{1}H NMR, in solution and in the agarose gel; they directly provide the value of $D_{i\subset\alpha-CD}^{[\alpha-CD]}$ for the concentration of α-CD in the investigated samples. The results are also given in Table 3.

In contrast to the preceding determination of the diffusion coefficients of the dyes, it is now necessary to obtain $D^0_{i\subset\alpha-CD}$ by correcting the $D_{i\subset\alpha-CD}^{[\alpha-CD]}$ from viscosity effect to compare the results given by both techniques. Hence, one obtains respectively $D^0_{1\subset\alpha-CD}$ (298 K) = 2.1 ± 1 × 10^{-10} m^2 s^{-1} and $D^0_{2\subset\alpha-CD}$ (283 K) = 0.9 ± 1 × 10^{-10} m^2 s^{-1} (direct observation), and $D^0_{1\subset\alpha-CD}$ (298 K) = 2.7 ± 0.07 × 10^{-10} m^2 s^{-1} and $D^0_{2\subset\alpha-CD}$ (283 K) = 1.4 ± 0.03 × 10^{-10} m^2 s^{-1} (gradient field ^{1}H NMR). These sets satisfactorily compare. In the following, we kept the more directly accessed values obtained from NMR experiments: $D^0_{1\subset\alpha-CD}$ (298 K) = 2.7 ± 0.07 10^{-10} m^2 s^{-1} and $D^0_{2\subset\alpha-CD}$ (283 K) = 1.4 ± 0.03 × 10^{-10} m^2 s^{-1}.

Calibration of the Electric Field. To analyze the forthcoming experimental results, eq 5 requires to determine the products $a\mu_i$ and $a\mu_{i\subset\alpha-CD}$ that identify to the species velocities v_i and $v_{i\subset\alpha-CD}$.

Provided that the mobilities of *i* are known, one could attempt to calibrate the field amplitude $a(U_{app})$ from observing the velocity of the dye as a function of the applied voltage U_{app}. The electrophoretic mobility μ generally obeys $\mu = \varphi zeD/k_B\theta$ where e designates the electron charge, k_B the Boltzmann constant, θ the absolute temperature, and φ a function depending on the ionic strength and on the species geometry.[56−58] We first attempted to use the values of z_i and D_i determined in the present study to calculate the mobilities μ_i. To evaluate the relevance

of such an approach, we measured the relative values φ/φ_{ref} at 0.15*M* ionic strength using fluorescein as a reference ($z_{ref} = 2$ at pH = 11 and $D_{ref} = 3.0 \times 10^{-10}$ m^2 s^{-1} [59]). We found $\varphi_1/\varphi_{ref} = 0.69$ and $\varphi_2/\varphi_{ref} = 0.75$. This departure from unity emphasized the difficulty to access to the electric reaction field created by the counterions of the charged species.

The latter result led us to only calibrate the dependence of the species velocities $v_i = a\mu_i$ on the applied voltage U_{app}. The results are given in Figure 7S. As anticipated, the velocities v_i are linearly related to U_{app}. The slopes provide apparent mobilities u_i that depends both on the intrinsic mobilities μ_i and on the geometry of the electrophoretic cell. Under the present experimental conditions ([**i**] = 0.3 mM, 1% agarose, pH = 12, $I = 0.15$ M), we obtained: u_1^0(298 K) $= 6.2 \times 10^{-7}$ m s^{-1} V^{-1}, u_1^0(283 K) $= 4.1 \times 10^{-7}$ m s^{-1} V^{-1}, u_2^0(298 K) $= 6.0 \times 10^{-7}$ m s^{-1} V^{-1}, and u_2^0(283 K) $= 4.0 \times 10^{-7}$ m s^{-1} V^{-1}.

The corresponding apparent mobilities $u^0_{i\subset\alpha-CD}$ of the $i \subset$ α-CD complexes were determined from the analysis of the dependence on α-CD concentration of the velocity $v_{\{i,i\subset\alpha-CD\}}$ of the front migration of the dyes **i**. As we did to derive the extrapolated values of the diffusion coefficients to [α-CD] = 0, the experimental data were corrected from the increase of the viscosity (eq 11) before fitting according to eq 12

$$v_{\{i,\, i\subset\alpha-CD\}}{}^{0} = \frac{1}{(K_i[\alpha\text{-CD}]+1)}v_i{}^{0} + \frac{K_i[\alpha\text{-CD}]}{(K_i[\alpha\text{-CD}]+1)}v_{i\subset\alpha-CD}{}^{0} \quad (12)$$

with K_i and $v^0_{i\subset\alpha-CD}$ as adjusting parameters, and using the values of $v_i^0(U_{app})$ obtained above (see Figure 4, parts a and b). The observed velocities $v_{\{i,i\subset\alpha-CD\}}$ satisfactorily obey eq 12. The extracted values for K_i are in agreement with the values extracted from titration followed by UV−vis absorption (vide supra) or from ^{1}H NMR (see Table 2). The corresponding fits were used to derive $u^0_{1\subset\alpha-CD}$ (298 K) $= 3.4 \times 10^{-7}$ m s^{-1} V^{-1}, and $u^0_{2\subset\alpha-CD}$ (283 K) $= 1.6 \times 10^{-7}$ m s^{-1} V^{-1}.

Measurement of the Effective Diffusion Coefficients. Once the preliminary experiments devoted to collect the relevant parameters were performed, the dispersion behaviors of the dyes i were investigated to evaluate the validity of the theoretical model exposed above. Three different issues were addressed: (i) the existence of a transition at which $D_{diff} = D_{disp}$ between weak-field and strong-field regimes for the electrical field; the dispersive behavior as a function of (ii) the period of the electric field and of (iii) the concentration in α-CD given in eq 5. Points i and ii were addressed for the dye **1** only, whereas point iii was illustrated for both dyes **1** and **2**.

Dependence upon Field Amplitude. The preliminary experiments provided direct access to the resonance conditions given in eq 8 for the dye **1** at 298 K: $[\alpha\text{-CD}]^R = 1/K_1 = 5.8$ mM and $T = 3.212/k_{1,2} = 90$ s. These parameters were chosen to investigate the dependence of the effective diffusion coefficient of 1 on the field amplitude in the 0−100 V range for the applied voltage U_{app}. The experimental data are displayed in Figure 5 together with the fit by eqs 2, 3, and 5, introducing the extrapolated values of D_1^0(298 K), $D^0_{1\subset\alpha-CD}$ (298 K), u_1^0(298 K), and $u^0_{1\subset\alpha-CD}$ (298 K) corrected from viscosity, and using $\kappa_{1,1}$(298 K) and $k_{1,2}$(298 K) as floating parameters. The fit is satisfactory and yields rate constants close to the expected values (see Tables 1 and 2). One observes two distinct regimes as anticipated from eq 2. For weak fields ($U_{app} < 10$ V), D_{eff} is controlled by Brownian motion; it is essentially independent of the field amplitude. At a larger electric field, D_{eff} is dominated by the dispersion term. The transition between the two regimes occurs over a small range ($\Delta U_{app} = 30V$) around $U_{app} = 55$ V. For the latter values, one observes $D_{eff} \simeq 2D_{dif}$ as predicted by eqs 2, 3, and 5.

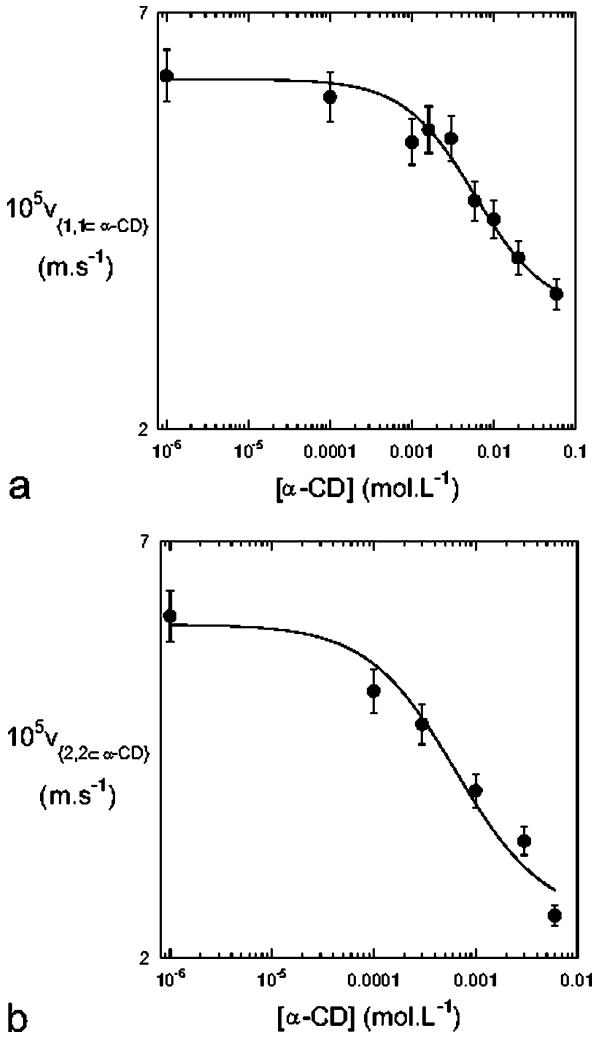

Figure 4. Dependence on α-CD concentration of the velocity $v_{\{i,i\subset\alpha-CD\}}$ of the front migration of the dyes **i** [(a) **i** = **1** θ = 298 K and (b) **i** = **2** θ = 283 K). The experimental data (circles) were corrected from viscosity using eq 11 before fitting according to eq 12. See the text.

Dependence upon Field Pulsation. The resonance conditions for the concentration in α-CD (298 K, $[\alpha\text{-CD}]^R = 1/K_1 = 5.8$ mM) were also chosen to investigate the significance of the field period on the dispersion behavior of **1**. The applied voltage was fixed to 100 V to be in the relevant regime of strong field. On the other hand, the applied voltage was limited to avoid any detrimental Joule effect on the gel. The lower value of the investigated range of frequencies was fixed to 5 mHz to prevent the concentration profile from leaving the recorded frame during the acquisition. The experimental points are given in Figure 6 together with the fit relying on eqs 2, 3, and 5, introducing the apparent mobilities u_1^0(298 K) and $u^0_{1\subset\alpha-CD}$ (298 K) corrected from the viscosity according to eq 11 and using $\kappa_{1,1}$(298 K) and $k_{1,2}$(298 K) as floating parameters. The agreement between the experimental results and the theoretical predictions is satisfactory (see Tables 1 and 2). At high frequency, the period of the field is much shorter than the average lifetimes of **1** and 1 ⊂ α-CD. In such a regime of slow chemical exchange, the amplitude of the field vanishes in average at the chemistry time scale; under such conditions, there is no coupling between

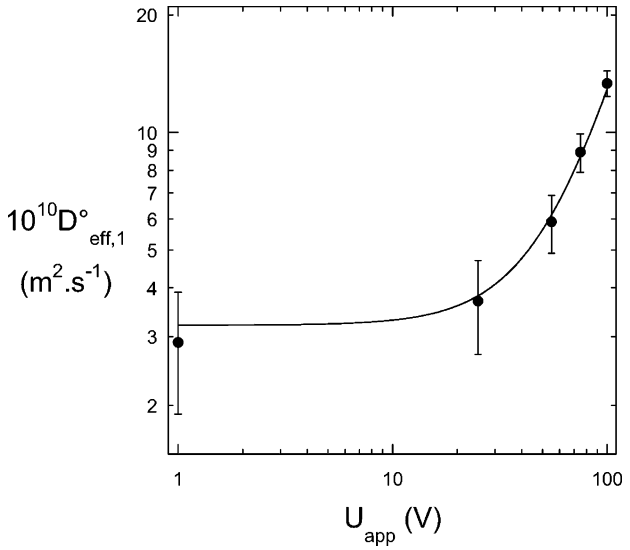

Figure 5. $\log_{10}-\log_{10}$ plot of the effective diffusion coefficients $D_{eff,1}$ at 298 K versus the applied voltage U_{app} which provides a periodic square wave electric field ($[\alpha\text{-CD}]^R = 1/K_1 = 5.8$ mM, $T = 3.212/k_{1,2} = 90$ s). The circles correspond to the experimental data. The solid line is obtained from fitting by eq 2. The floating parameters are $\kappa_{1,1}$ and $k_{1,2}$, and all of the other parameters take the values determined by the present study. See the text.

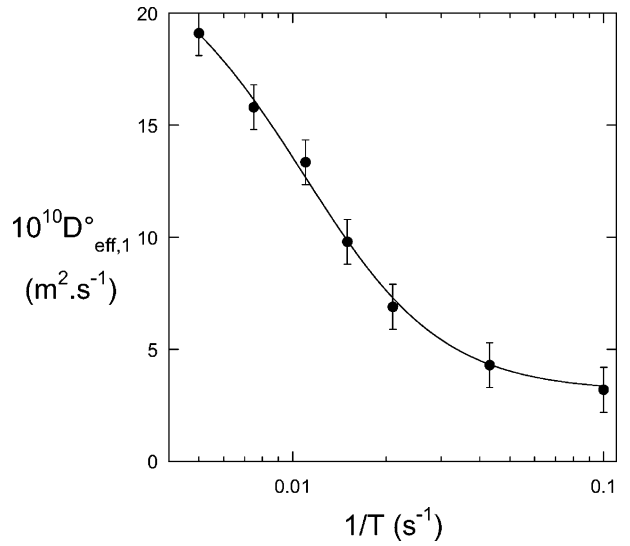

Figure 6. Variation of the effective diffusion coefficients $D_{eff,1}$ at 298 K with the frequency $1/T$ of the square wave electric field at an applied voltage $U_{app} = 100$ V ($[\alpha\text{-CD}]^R = 1/K_1 = 5.8$ mM). The circles correspond to the experimental data. The solid line is obtained from fitting by eq 2. The floating parameters are $\kappa_{1,1}$ and $k_{1,2}$, and all of the other parameters take the values determined during the present study. See the text.

chemistry and the electric field. At low frequency, the chemical exchange between **1** and $1 \subset \alpha$-CD is fast at the time scale of the periodically altered electric field. As the frequency decreases, D_{eff} tends to the limit value of constant field which is not reached because of the experimental limitations exposed above.

Dependence upon α-CD Concentration. In relation to Figure 1b, one is eventually concerned with investigating the dispersion behavior of the dyes as a function of the concentration in α-CD for a fixed period of the alternating electric field chosen equal to its resonance value given in eq 8 (90*s* for **1** at 298*K* and 31*s* for **2** at 283*K*). To obtain the maximal amplitude for the dispersion while limiting heat release by Joule effect, the applied voltage was made as high as possible ($U_{app} = 100V$ for **1** at 298*K* and $U_{app} = 150V$ for **2** at 283*K*). The study was performed over a large range of α-CD concentrations extending from 0*M* to 5.8 $10^{-2}M$ for **1**, and 6.0 $10^{-3}M$ for **2**. Figures 7a and 7b display the experimental results together with the fits relying on eqs 2, 3, 5 introducing the extrapolated values of D_i^0, $D_{i\subset\alpha-CD}^0$, u_i^0, and $u_{i\subset\alpha-CD}^0$ with the viscosity correction given in eq 11. $\kappa_{i,1}$ and $k_{i,2}$ were used as floating parameters. The corresponding fits satisfactorily compare with the experimental results for both dyes (see Tables 1 and 2). Two points are especially significant: (i) the maximum of the dispersion coefficient obeys the resonance condition expressed in eq 8 ($[\alpha\text{-CD}]^{D_{eff,1,max}} = [\alpha\text{-CD}]^{R,1} = 5.8$ mM for **1** and $[\alpha\text{-CD}]^{D_{eff,2,max}} = [\alpha\text{-CD}]^{R,2} = 1$ mM for **2**); (ii) the amplitude of the phenomenon is reproduced. As anticipated from eqs 2, 3, and 5, one obtains a purely diffusive behavior at low and large concentration in α-CD.

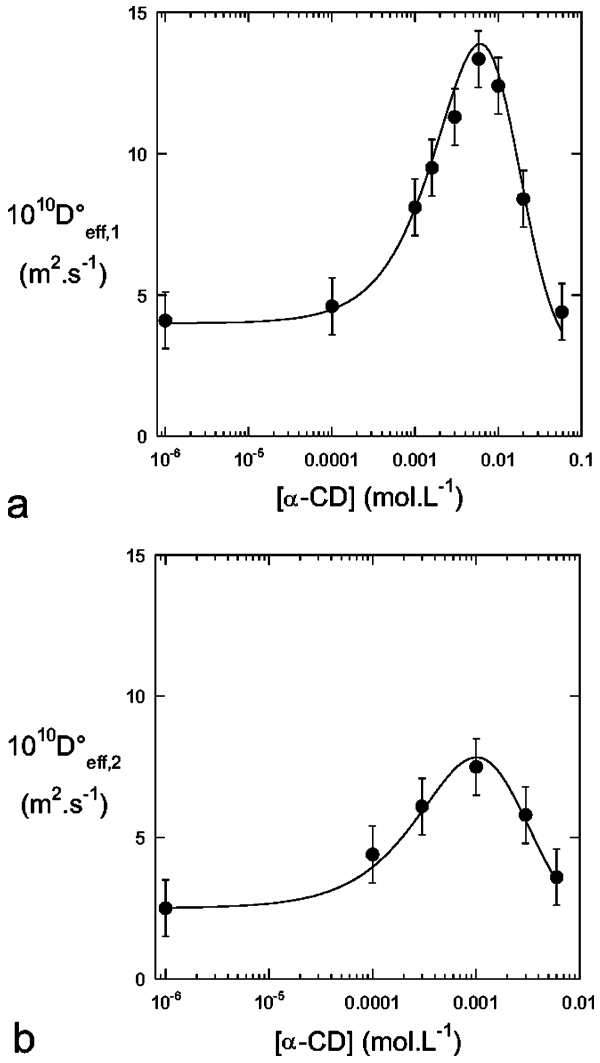

Figure 7. Variation of the effective diffusion coefficients $D_{eff,i}$ with the concentration in α-CD. The circles correspond to the experimental data. The solid line is obtained from fitting by eq 2. The floating parameters are $\kappa_{1,1}$ and $k_{1,2}$, and all of the other parameters are given by the values determined during the present study. (a) $\mathbf{i} = \mathbf{1}$, $\theta = 298$ K, $T = 90$ s, $U_{app} = 100$ V; (b) $\mathbf{i} = \mathbf{2}$, $\theta = 283$ K, $T = 31$ s, $U_{app} = 150$ V.

The similarity of the values of the rate constants $k_{1,1}$ and $k_{1,2}$ extracted from the three independent sets of experiments, as well as the agreement between the experimental and the theoretical behavior can be considered to support the theoretical model exposed above.

4. Conclusion

The present work demonstrates that the effective diffusion coefficient of a field-sensitive reactant can be considerably enhanced without introducing any observable mean displacement. Such a phenomenon can be obtained by applying a periodic external field with null average amplitude on the reactive medium. The increase is the most pronounced when specific relations involving the rate constants and the period of the field are fulfilled. The selectivity of this behavior is interpreted as resulting from a stochastic resonance implying the hopping process between the reactants and the products, and the alternating field.

The present dispersion phenomenon could find useful applications in Chemistry. For instance, the rate constants for dye complexations by α-CD were obtained from stop-flow experiments that require a rather expensive equipment. The approach reported in this paper provides an alternative method to determine rate constants. One could also use this phenomenon to perform separations within a mixture of similar species only differing by the values of their rate constants as suggested in our previous theoretical paper[21] and preliminary account.[45]

5. Experimental Section

Chemicals. α-CD and fluorescein were respectively purchased from Avocado and Fluka. The azo dyes were synthesized according to classical procedures.[60] The low electroendosmosis agarose was obtained from Roche. The Britton-Robinson buffers were prepared according to ref 61.

UV/vis Spectroscopic Measurements. The UV/vis absorption spectra were recorded on a Kontron Uvikon-940 spectrophotometer at the suitable temperature.

The protonation constant of the dyes **i** were obtained by following the evolution of the absorption spectrum of a 2×10^{-5} M solution of **i** in pH = 12 buffer (ionic strength 0.15 M) by 0.2 M HCl (Figures 1S and 2S). At a given wavelength λ, the absorbance A_λ from the solution contained in a 1*cm* cuvette obeys eq 13

$$A_\lambda = [A^-]\left(\epsilon_{AH}(\lambda)\frac{10^{-pH}}{K_{a,2}(i)} + \epsilon_{A^-}(\lambda)\right) \quad (13)$$

and the ratio $A_{\lambda_1}/A_{\lambda_2}$ eq 14

$$\frac{A_{\lambda_1}}{A_{\lambda_2}} = \frac{\epsilon_{AH}(\lambda_1)10^{-pH} + \epsilon_{A^-}(\lambda_1)K_{a,2}(\mathbf{i})}{\epsilon_{AH}(\lambda_2)10^{-pH} + \epsilon_{A^-}(\lambda_2)K_{a,2}(\mathbf{i})} \quad (14)$$

$pK_{a,2}$ was eventually derived from fitting the ratiometric measurement A_{390nm}/A_{424nm} for **1** and A_{380nm}/A_{420nm} for **2** as a function of pH according to eq 14 (see Figures 1Sb and 2Sb).

The α-CD: **i** association constants K_i were evaluated from titration of **i** by a mixed solution of α-CD and **i**, at constant concentration $[\mathbf{i}]_{tot}$ in **i** (Figures 3S and 4S). The absorbance $A_{\lambda exc}([CD])$ was analyzed from eq 15[62]

$$A_{\lambda exc}([CD]) = A_{\lambda exc}(0) - \frac{A_{\lambda exc}(0) - A_{\lambda exc}(\infty)}{2} \times \left\{\left(1 + x + \frac{1}{K_i[i]_{tot}}\right) - \sqrt{\left(1 + x + \frac{1}{K_i[i]_{tot}}\right)^2 - 4x}\right\} \quad (15)$$

where $A_{\lambda exc}(0)$ and $A_{\lambda exc}(\infty)$ are the initial and the asymptotic limits of the absorbance at λ_{exc}, and x is the ratio $[CD]_{tot}/[\mathbf{i}]_{tot}$ (Figures 3Sb and 4Sb).

^{1}H-HMR. *Sample Preparation.* Three different types of samples were prepared for NMR measurements. Three references samples, I, II_1, and II_2, were devoted to access the intrinsic diffusion coefficients of α-CD, and of the dyes **1** and **2**. They respectively contained α-CD, **1** and **2** at 5 mM in D_2O at pH = 12 and 0.15 M ionic strength after suitable addition of KOD and NaCl. Two other samples, III_1 and III_2, were similarly prepared to derive the diffusion coefficient of 1 ⊂ α-CD ([**1**] = 5 mM, [α-CD] = 8.3 mM) and 2 ⊂ α-CD ([**2**] = 5 mM, [α-CD] = 1 mM); pH = 12; NaCl = 0.15 M.

Evaluation of an Order of Magnitude for the Association Constants K_i. The average of the integrals corresponding to the free dye **i** and to the bound dye i ⊂ α-CD were measured in the samples III_1 and III_2 by recording their ^{1}H NMR spectrum. Then the K_i were evaluated by applying conservation laws.

Measurement of Diffusion Coefficients by Gradient Field ^{1}H NMR. The measurements of translational diffusion coefficients were carried out on an Avance Bruker DRX 600 spectrometer equipped with a TBI probe with three orthogonal gradient coils. The pulse sequence used was a double stimulated echo (DSTE) which suppresses the effects of fluid velocity (convection).[63] Eddy current effects were minimized using sine shaped pulsed field gradients (PFG) and introducing a longitudinal eddy current delay (LED) of 5 ms before acquisition. Encoding and decoding gradients were applied along the same axis as the static field while cleaning gradients at the beginning of every longitudinal period were applied along orthogonal axes. The total diffusion delays were 200 ms to measure the diffusion coefficient of solvent protons and 400 ms for every other experiment. Encoding PFG lengths were of 1 ms for solvent proton diffusion, 1.2 ms for the dye experiment and 2 ms for the experiments performed on α-CD and the α-CD:dye complex. Their maximum amplitudes were varied from 5.6 G cm^{-1} to 52.9 G cm^{-1} in 32 steps. The solvent proton experiment required only 8 transients for every sample while the number of transients were varied from 8 to 32 to give appropriate signal-to-noise ratios in samples containing either the dye or the cyclodextrin. Finally, 64 scans were recorded for the sample "in solution" and 128 in the gel. Assignments of the signals of the different species in solution were carried out by direct comparison of the spectra of the dye alone, the α-CD alone and the mixed sample. This very slow exchange regime enabled us to measure the diffusion of all species in the mixed sample. Only nonoverlapping signals were employed to obtain the expected decay curves. The decays of the amplitude of the echo with increasing gradient strength were fitted using the expression[63]

$$S = S_0 \exp(-\gamma^2 g^2 \delta^2 D(\Delta + 2\delta/3)) \quad (16)$$

where S_0 is the echo amplitude with vanishing gradients; γ, the gyromagnetic ratio of the protons; g, the effective amplitude of the gradients; δ, the duration of the gradients; Δ, the delay between encoding and decoding gradients; and D, the diffusion coefficient of the molecule under study.

For dye **2**, a second series of experiments was carried out on an Avance Bruker DRX 400 wide bore spectrometer equipped with a TXI probe with a *z*-axis gradient coil. We only report the experimental parameters different from the study described above. Encoding PFG length was 3 ms in all experiments. The maximum amplitude of the gradients was varied from 5.8 G cm^{-1} to 55.1 G cm^{-1} in 16 steps. The total diffusion delay was set to 150 ms for the diffusion of the dye alone and 200 ms for samples containing the α-CD. The number of scans was varied from 32 to 128 for measurements in solution and between 64 and 256 for measurements in the gel.

Dependence of Solution Viscosity on α-CD Concentration. *Evaluation by Measurement of Current Intensity.* The current intensity I in the electrophoretic cell obeys eq 17

$$I = aFS\sum_i z_i\mu_i c_i \tag{17}$$

where $F = 96500$ C, S designate the gel cross-section, z_i and c_i are respectively the charge and the concentration of the ion i. At 0.15 M ionic strength, the dyes do not play any significant role in the current that mainly results from motions of buffer ions whose mobilities μ_i are inversely proportional to the medium viscosity. One obtains eq 10.

The relevant data were collected during the series of experiments devoted to determine the dependence of the effective diffusion coefficients of the dyes on α-CD concentration. For a $1 \times 1 \times 30$ mm^3 capillary filled with the 1% agarose gel at pH = 12 and 0.15 M, the current intensity delivered by the power supply varies from $I = 3.1$ mA at [α-CD] = 0 M to $I = 2.4$ mA at [α-CD] = 0.058 M.

Evaluation by Fluorescence Correlation Spectroscopy (FCS). The diffusion coefficient of fluorescein $D^*([CD])$ was measured by FCS as a function of the concentrations in α-CD. In fact, the diffusion coefficient and the medium viscosity are linked by a relation of type (18)[56]

$$D^* = \frac{k_B\theta}{f} \tag{18}$$

where k_B is the Boltzmann constant, θ the absolute temperature and f a friction factor linearly related to medium viscosity (for instance, $f = 6\pi\eta R$ for a freely diffusing sphere of radius R). Thus, one obtains eq 10.

The diffusion coefficient can be extracted from FCS experiments as follows. In a three-dimensional Gaussian excitation profile characterized by two distances ω_{xy} (beam-waist) and ω_z ($I = I_0 \exp[-2(x^2 + y^2)/\omega_{xy}^2 - 2z^2/\omega_z^2]$; $\rho = \omega_z/\omega_{xy}$), the correlation function $G(\tau)$ of the fluctuation of the fluorescence intensity I_F (eq 19)

$$G(\tau) = \frac{\langle\delta I_F(t)\delta I_F(t+\tau)\rangle}{\langle I_F\rangle^2} \tag{19}$$

originating from a freely diffusing fluorescent species (average concentration = $\langle C\rangle$) obeys eq 20

$$G(\tau) = \frac{1}{\langle C\rangle V}\frac{1}{\left(1+\frac{\tau}{\tau_D}\right)}\frac{1}{\left(1+\rho^2\frac{\tau}{\tau_D}\right)^{0.5}} \tag{20}$$

where τ_D designates the diffusion time of the species through the excitation profile (volume V).

Provided that ω_{xy}, ρ and the illuminated volume $V \simeq \pi\omega_{xy}^4/\lambda$ (λ = excitation wavelength) can be calibrated, the fitted experimental $G(\tau)$ curves gives access to D^* thanks to the relation $\tau_D = \omega_{xy}^2/8D^*$ that applies for two-photon excitation. Our two-photon excitation FCS setup was described elsewhere.[64] Using fluorescent beads of 27 nm radius filled with fluorescein (Molecular Probes) for calibration, we found $\omega_{xy} \simeq 0.3$ μm and $\rho^2 \simeq 0.01$.

During the present series of experiments, we observed that $G(\tau = 0)$ decreased at large concentrations of α-CD. We checked that the latter observation was not related to any significant change of refractive index; we correspondingly assumed light diffusion to expand the excitation profile without strongly altering its geometry ($G(\tau = 0)$ is inversely proportional to V). To correct for a change in ω_{xy}, we eventually determined $\eta([CD])/\eta([CD] = 0)$ from eq 21

$$\frac{\eta([CD])}{\eta([CD]=0)} = \frac{D^*([CD]=0)}{D^*([CD])} = \frac{\tau_D([CD])\sqrt{G(\tau=0,[CD])-1}}{\tau_D([CD]=0)\sqrt{G(\tau=0,[CD]=0)-1}} \tag{21}$$

Measurement of the Diffusion Coefficients and of the Velocities by Microscopic Observation. *Experimental Set Up.* The measurements were performed in a small transparent electrophoretic cell (Figure 3). Two reservoirs containing the platinum electrodes are linked by a 1×1 mm^2 square glass capillaries (VitroCom) immersed in a thermostated transparent glass cell (in the relevant regime of applied voltages U_{app}, the linear behavior observed in Figure 7S demonstrates that the heat produced by Joule effect was efficiently transferred to the thermostat). The capillary is observed by transmission. The dye absorbs the light from a blue light emitting diode (Silicon Carbide blue LED) and the remaining light is collected with a CCD camera (COHV 4913) connected to a computer. The observed field is about 20 mm with a spatial resolution equal to 34 ± 0.5 μm pixel^{-1}.

Experimental Protocol. The capillary is filled with a hot (>88 °C) 1%(m/m) agarose solution prepared by dissolving the agarose powder in the Britton-Robinson pH = 12 buffer at 0.15 mol L^{-1} possibly containing α-CD at the suitable concentration. After gelation, the capillary is mounted in the electrophoretic cell and the electrode reservoirs are filled with the Britton-Robinson pH = 12 buffer at 0.15 mol L^{-1} with the same α-CD concentration as in the gel. One reservoir is adjusted at 3×10^{-4} M in dye. Then a constant electric field is applied with a d.c. voltage generator (CONSORT-E385) to bring the concentration step of dye in the middle of the capillary. At that step, the constant electric field is either turned out, or changed into an alternative field depending on purpose. The frequency of the square wave field is driven by the data acquisition program which allows synchronous detection.

Data Processing. The experimental setup allows three-dimensional diffusion of the chemical species. Nevertheless the strong anisotropy of the capillary causes a much faster relaxation of concentration heterogeneities along the two axes that are perpendicular to the long axis of the capillary (a few minutes to compare to the whole duration of an experiment typically exceeding 1 h). As a consequence, diffusion can be considered to essentially occur in one dimension under the present experimental conditions.

The absorbed light in the recorded image is proportional to the concentration of absorbing species under the present experimental conditions. The derivation operators are linear, so that the image can be directly processed as if the gray levels express the concentrations of dyes. The diffusion coefficients were extracted from a spatial Fourier analysis of the image (Figure 6S). When the initial profile is a step function, the computer program first derivates along x the image and may stack the derivatives by correcting them from a possible migration. Then the one and only phenomenon to analyze is the diffusion of the (**i**, $i \subset$ α-CD) species the concentration profile of which obeys

$$\frac{\partial C_i(x,t)}{\partial t} = D_{eff,i}\frac{\partial^2 C_i(x,t)}{\partial x^2} \tag{22}$$

Using a discrete Fourier transform, the preceding equation transforms into

$$\frac{\partial \tilde{C}_i(q, t)}{\partial t} = -D_{\mathrm{eff},i} q^2 \tilde{C}_i(q, t) \qquad (23)$$

with $q = 2\pi n/L$ where L designates the width of the acquisition window and n the index of the Fourier mode. Its solution is

$$\tilde{C}(q, t) = \tilde{C}(q, 0)\, \mathrm{e}^{-D_{\mathrm{eff},i} q^2 t} = \tilde{C}_{\mathrm{i}}(q, 0)\, \mathrm{e}^{-t/\tau_{\mathrm{n}}} \qquad (24)$$

with $\tau_n = 1/[D_{\mathrm{eff},i}(2\pi n/L)^2]$. The decays of the Fourier modes are fitted by an exponential law to extract the $1/\tau_n$ values. The quadratic dependence of $1/\tau_n$ on n provides the effective diffusion coefficient $D_{\mathrm{eff},i}$.

The migration velocity is directly measured by the observation of the location of the front of the concentration step as a function of time. To verify the stability of the electric field and of the temperature, the curve representing the front position as a function of time was derivated providing both the average value of the velocity and its standard deviation.

Acknowledgment. Hervé Lemarchand and David Bensimon are gratefully acknowledged for fruitful discussions. This work was supported by a special grant from the French ministry of research in the frame of the Action Concertée Incitative "Physicochimie de la matière complexe 2000".

Supporting Information Available: Seven Figures (1S: determination of p$K_{a,2}$(**1**); 2S: determination of p$K_{a,2}$(**2**); 3S: determination of K_1; 4S: determination of K_2; 5S: relative dependence of medium viscosity as a function of α-CD concentration; 6S: data processing to access to the velocity and to the diffusion coefficients of the dyes; 7S: dependence of the velocity v_i of the dyes **1** and **2** on the applied voltage U_{app}; 8S: theoretical variation in the normalized dispersion coefficient $D_{\mathrm{disp}}/[a(\mu_{\mathrm{C}} - \mu_{\mathrm{Q}})]^2$ of species (C, Q) submitted to a rectangular wave periodic field), one Table (1S: diffusion coefficients of water (*HOD*), α-CD, the dyes **i** and of the complexes i ⊂ α-CD in solution and in 1% agarose gel (in brackets) at 298 K (**i** = **1**) and at 283 K (**i** = **2**) as measured by gradient field ^{1}H NMR), and the theoretical analysis. This material is available free of charge via the Internet at http://pubs.acs.org.

References and Notes

(1) Guggenheim, E. A. *Thermodynamics*, 8th ed.; North-Holland: Amsterdam, 1987.

(2) Bockris, J. O'M.; Bockris, J. O.; Gambora-Aldeco, M. *Modern Electrochemistry: Ionics*, 2nd ed.; Plenum Publishing Corporation: New York, 1998.

(3) Bockris, J. O'M.; Gambora-Aldeco, M.; Reddy, A. K. N. *Modern Electrochemistry: Electrodics in Chemistry, Engineering, Biology, and Environmental Science*, 2nd ed.; Plenum Publishing Corporation: New York, 2000.

(4) Eigen, M.; de Mayer, L. Relaxation Methods. In *Techniques of Organic Chemistry*, 2nd ed.; Friess, S. L., Lewis, E. S., Weissberger, A., Eds.; Interscience Publishers: John Wiley and Sons: New York, 1963; Vol. VIII, Part II, pp 895−1054.

(5) Leffler, J. E.; Grunwald, E. *Rates and Equilibria of Organic Reactions as Treated by Statistical, Thermodynamic, and Extrathermodynamic Methods*; Dover: New York, 1989.

(6) Debye, P. *Ber. Deut. Physik. Ges.* **1913**, *15*, 777−793.

(7) One should here notice that chromatography has been marginally used to measure rate constants of chemical reactions along the same principle. In such experiments, one observes merging of the peaks corresponding to exchanging species by decreasing the velocity of the mobile phase. The corresponding experiments do not involve application of a periodic field but they similarly deal with a static field in a transient regime. See for instance: Stevens, F. J. *Biophys. J.* **1989**, *55*, 1155−1167.

(8) Wien, M.; Schiele, J. *Z. Phys.* **1931**, *32*, 545−547.

(9) Onsager, L. *J. Chem. Phys.* **1934**, *2*, 599−615.

(10) Eigen, M.; Schoen, J. *Z. Elektrochem.* **1955**, *59*, 483−494.

(11) Hu, G.; Nicolis, G.; Nicolis, C. *Phys. Rev. A* **1990**, *42*, 2030−2041.

(12) Gammaitoni, L.; Hänggi, P.; Jung, P.; Marchesoni, F. *Rev. Mod. Phys.* **1998**, *70*, 223−287.

(13) Leonard, D. S.; Reichl, L. E. *Phys. Rev. E* **1994**, *49*, 1734−1737.

(14) Dykman, M. I.; Horita, T.; Ross, J. *J. Chem. Phys.* **1995**, *103*, 966−972.

(15) Guderian, A.; Dechert, G.; Zeyer, K.-P.; Schneider, F. W. *J. Phys. Chem.* **1996**, *100*, 4437−4441.

(16) Amemiya, T.; Ohmori, T.; Yamamoto, T.; Yamaguchi, T. *J. Phys. Chem. A* **1999**, *103*, 3451−3454.

(17) Forster, A.; Merget, M.; Schneider, F. W. *J. Phys. Chem.* **1996**, *100*, 4442−4447.

(18) Hohmann, W.; Muller, J.; Schneider, F. W. *J. Phys. Chem.* **1996**, *100*, 5388−5392.

(19) van den Broeck, C. *Physica A* **1990**, *168*, 677−696.

(20) Claes, I.; van den Broeck, C. *Phys. Rev. A* **1991**, *44*, 8, 4970−4977.

(21) Jullien, L.; Lemarchand, A.; Lemarchand, H. *J. Chem. Phys.* **2000**, *112*, 8293−8301.

(22) Jullien, L.; Lemarchand, A.; Lemarchand, H. "Procédé de séparation d'un composé chimique ou biologique dans un mélange de composés similaires par diffusion dans un milieu tel qu'un gel", No. FR 99 133 66, 26/10/1999; No. PCT/FR 00/02974, 25/10/2000.

(23) Giddings, J. C.; Eyring, H. *J. Phys. Chem.* **1955**, *23*, 344−350.

(24) Giddings, J. C. *J. Chem. Phys.* **1957**, *26*, 169−173.

(25) Beynon, J. H.; Clough, S.; Crooks, D. A.; Lester, G. R. *Trans. Faraday Soc.* **1958**, *54*, 705−714.

(26) McQuarrie, D. A. *J. Chem. Phys.* **1963**, *38*, 437−445.

(27) Carmichael, J. B. *J. Polym. Sci. Part A-2*, **1968**, *6*, 517−527.

(28) Carmichael, J. B. *Macromolecules* **1968**, *1*, 526−529.

(29) Carmichael, J. B. *Polym. Prepr.* **1968**, *9*, 572−577.

(30) Carmichael, J. B. *Biopolymers* **1968**, *6*, 1497−1499.

(31) Weiss, G. H. *Sep. Sci.* **1970**, *5*, 51−62.

(32) Phillips, J. B.; Wright, N. A.; Burke, M. F. *Sep. Sci. Technol.* **1981**, *16*, 861−884.

(33) Weiss, G. H. *Sep. Sci. Technol.* **1982**, *17*, 1609−1622.

(34) Scott, D. M.; Fritz, J. S. *Anal. Chem.* **1984**, *56*, 1561−1566.

(35) Schure, M. R. Particle Simulation Methods in Separation Science. In *Advances in Chromatography*; Brown, P. R., Grushka, E., Eds.; Marcel Dekker: New York, 1998; Vol. 39, pp 139−200.

(36) Dondi, F.; Munari, P.; Remelli, M.; Cavazzini, A. *Anal. Chem.* **2000**, *72*, 4353−4362.

(37) Cavazzini, A.; Dondi, F.; Jaulmes, A.; Vidal-Madjar, C.; Felinger, A. *Anal. Chem.* **2002**, *74*, 6269−6278.

(38) Van Kampen, N. G. *Physica* **1979**, *96A*, 435−453.

(39) Dondi, F.; Cavazzini, A.; Remelli, M.; Felinger, A.; Martin, M. *J. Chromatogr. A* **2002**, *943*, 185−207.

(40) Yarmola, E.; Calabrese, P. P.; Chrambach, A.; Weiss, G. H. *J. Phys. Chem. B* **1997**, *101*, 2381−2387.

(41) Jandera, P.; Backobska, W.; Felinger, A. *J. Chromatogr. A* **2001**, *919*, 67−77.

(42) Pasti, L.; Dondi, F.; van Hulst, M.; Schoenmakers, P. J.; Martin, M.; Felinger, A. *Chromatographia* **2003**, *75*, 171−186.

(43) Mysels, K. J. *J. Chem. Phys.* **1956**, *24*, 371−375.

(44) Giddings, J. C. *J. Chem. Phys.* **1957**, *26*, 1755−1756.

(45) Alcor, D.; Croquette, V.; Jullien, L.; Lemarchand, A. *Proc. Natl. Acad. Sci. U.S.A.* **2004**, *101*, 8276−8280.

(46) The case of an asymmetric rectangular wave electric field is analyzed in the Supporting Information.

(47) Cramer, P.; Saenger, W.; Spatz, H.-C. *J. Am. Chem. Soc.* **1967**, *89*, 1−20.

(48) Yoshida, N.; Seiyama, A.; Fujimoto, M. *J. Phys. Chem.* **1990**, 4246−4253.

(49) Yoshida, N. *J. Chem. Soc., Perkin Trans. 2* **1995**, 2249−2256.

(50) Abou-Hamdan, A.; Bugnon, P.; Saudan, C.; Lye, P. G.; Merbach, A. E. *J. Am. Chem. Soc.* **2000**, *122*, 592−602.

(51) Kortüm, G.; Vogel, W.; Andrussow, K. *Dissociation Constants of Organic Acids in Aqueous Solution*; Butterworths: London, 1961.

(52) Tanford, C.; Kirkwood, J. G. *J. Am. Chem. Soc.* **1957**, *79*, 5333−5339.

(53) Jullien, L.; Cottet, H.; Hamelin, B.; Jardy, A. *J. Phys. Chem. B* **1999**, *103*, 10866−10875.

(54) Gelb, R. I.; Schwartz, L. M.; Bradshaw, J. J.; Laufer, D. A. *Biorg. Chem.* **1980**, *9*, 299−304.

(55) Pernodet, N.; Maaloum, M.; Tinland, B. *Electrophoresis* **1997**, *18*, 55−58.
(56) Cantor, C. R.; Schimmel, P. R. *Biophysical Chemistry*; Freeman: New York, 1980; Part II.
(57) Rice, S. A.; Nagasawa, M. *Polyelectrolyte Solution, A Theoretical Introduction*; Academic Press: New York, 1961.
(58) Henry, D. C. *Proc. R. Soc.* **1931**, *A133*, 106−129.
(59) Chen, Y.; Chen, Y.; Müller, J. D.; Eid, J. S.; Gratton E. In *New Trends in Fluorescence Spectroscopy*; Valeur, B., Brochon, J. C., Eds.; Spinger : New York, 2001.
(60) *Vogel's Textbook of Practical Organic Chemistry*, 4th ed.; Longman: London, 1978.
(61) Frugoni, C. *Gazz. Chim. Ital.* **1957**, *87*, 403−407.
(62) See for instance: Jullien, L.; Canceill, J.; Valeur, B.; Bardez, E.; Lefèvre, J.-P.; Lehn, J.-M.; Marchi-Artzner, V.; Pansu, R. *J. Am. Chem. Soc.* **1996**, *118*, 5432−5442.
(63) Jerschow, A.; Muller, N. *J. Magn. Reson.* **1997**, *125*, 372−375.
(64) Gosse, C.; Boutorine, A.; Aujard, I.; Chami, M.; Kononov, A.; Cogné-Laage, E.; Allemand, J.-F.; Li, J.; Jullien, L. *J. Phys. Chem. B* **2004**, *108*, 6485−6497.